



มหาวิทยาลัยมหิดล  
Mahidol University

## รายงานวิจัยฉบับสมบูรณ์

โครงการ การพัฒนาสารสិទ្ធិអំពីការបង្កើតការងារ  
នៃប្រព័ន្ធគ្រប់គ្រងការងារ នៃប្រព័ន្ធគ្រប់គ្រងការងារ  
នៃប្រព័ន្ធគ្រប់គ្រងការងារ នៃប្រព័ន្ធគ្រប់គ្រងការងារ

โดย ดร.นพพร เรืองสุภาภิชาติ

เดือนธันวาคม ปี 2560 ที่เสร็จโครงการ

สัญญาเลขที่ TRG5880110

## รายงานวิจัยสนับสนุนบูรณา

โครงการ การพัฒนาสารสืบย้อมสังเคราะห์ที่ดูดกลืนแสง  
ในช่วงคลื่นอินฟราเรดสำหรับเซลล์แสงอาทิตย์โดยใช้  
โครงสร้างหลักเป็นสารอินโดโล-อินโดล

ผู้วิจัย ดร.นพพร เรืองสุภาภิชาติ สังกัดมหาวิทยาลัยมหิดล

สนับสนุนโดยสำนักงานกองทุนสนับสนุนการวิจัยและ  
ต้นสังกัด

(ความเห็นในรายงานนี้เป็นของผู้วิจัย  
สกอ.และต้นสังกัดไม่จำเป็นต้องเห็นด้วยเสมอไป)

**Abstract :** Three organic dyes containing a nitrogen-bridged phenylenevinylene (NPV: indolo[3,2-*b*]indole) unit were synthesized and applied in dye-sensitized solar cells, where NPV was employed as a donor itself or as a  $\pi$ -spacer with the extra-donor diphenylamine. The photophysical, electrochemical and photovoltaic properties of the dyes were investigated. All dyes displayed broad absorption spectra and high molar extinction coefficient, resulting in high light harvesting efficiency. The results showed that the dye with two cyanoacrylic acid as the acceptors exhibited photovoltaic performance of 7.39% under standard global AM 1.5 solar condition, better than the other two with only one acceptor. These results indicate that the NPV-based organic dye is a promising candidate for efficient DSSCs.

**รูปแบบบทคัดย่อ :** การนำพลังงานจากแสงอาทิตย์มาใช้แทนการใช้พลังงานจากเชื้อเพลิงเป็นเป้าหมายหลักของการวิจัยนี้ การพัฒนาสารสีข้อมโนเลกุลใหม่ที่มีความแตกต่างและมีความสามารถในการดูดซับพลังงานแสงอาทิตย์ในช่วงความยาวคลื่นใกล้เคียงกับแสงอินฟราเรด (NIR) เพื่อใช้ในเซลล์แสงอาทิตย์ โดยการออกแบบและสังเคราะห์อนุพันธ์ใหม่ของโนเลกุลที่มีอินโดโล-อินโคล เป็นสารโครงสร้างหลัก เนื่องจากสาร NPV (indolo[3,2-*b*]indole) มีคุณสมบัติทางกายภาพที่ยอดเยี่ยม เช่น ความทนทานและการดูดกลืนแสงที่ดี โดยการสังเคราะห์สารสีข้อมนี้ได้ถูกสังเคราะห์ออกแบบตามตัวอย่าง พร้อมทั้งศึกษาสมบัติทางแสงและไฟฟ้าของสารสีข้อมทั้งสามตัว พบว่าสารสีข้อมทั้งหมดแสดงสเปกตรัมการดูดกลืนแสงในช่วงกว้างและมีค่าสัมประสิทธิ์การดูดกลืนแสงที่สูงทำให้มีประสิทธิภาพในการเก็บเกี่ยวแสงอาทิตย์สูง นอกจากนี้สารทั้งสามยังได้ถูกนำมาขึ้นรูปเป็นเซลล์แสงอาทิตย์ และพบว่าเซลล์แสงอาทิตย์ที่ใช้สารสีข้อมนี้ในตัวดังกล่าวมีประสิทธิภาพการทำงานสูงถึง 7.39%

---

**Project Code :** TRG5880110

(รหัสโครงการ)

**Project Title :** NIR organic sensitizer based on dihydroindolo[3,2-*b*]indole structure for dye-sensitized solar cells

(ชื่อโครงการ)

**Investigator :** Nopporn Ruangsupapichat, Department of Chemistry, Faculty of Science, Mahidol University

(ชื่อหัววิจัย)

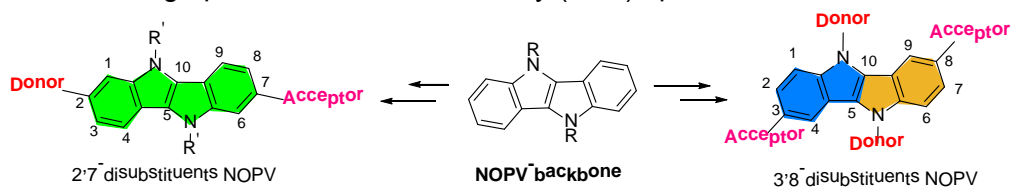
**E-mail Address :** Nopporn.rua@mahidol.ac.th

**Project Period :** 2 years and 6 months

(ระยะเวลาโครงการ)

## Executive summary

The main goals of this research are not only to design and study new dyes with a  $\pi$ -conjugated nitrogen-bridge oligomer phenylenevinylene (NPV) backbone, but also to achieve the high power conversion efficiency (PCE) up to 8%.



The synthesis and application of oligomer phenylenevinylene derivatives have been developed and beneficial to material science because these compounds are quite interesting due to their intrinsic photophysical and redox properties. In addition, there are more advantages of this building block: 1) shorter synthetic route, 2) similar  $\pi$ -conjugated as phenylenevinylene system, 3) easy functionalize substituents to specific positions on *N,N'*-positions which can be achieved high mobility and morphology of molecules on solid-state, 4) importantly, there are no scientific papers using this core for organic solar cells so far. Thus this new core nitrogen-bridge oligomer phenylenevinylene (indolo-indole) will be synthesized and further introduced to optoelectronic devices.

Two types of indolo-indole have been synthesized and been ready to functionalize as organic dyes for optoelectronic and solar cell applications. Photophysical properties of indolo-indole have been studied. With their great physical properties such as robustness, excellent photostability, and high carrier mobility, these dyes will be promising as sensitizers. In the final process, a solar cell device using one of these functionalized dihydroindolo [3,2-*b*]indole (NOPV) molecules as a photoexcitable donor were fabricated and one of them exhibits the maximum power conversion efficiency of 7.39% ( $J_{sc} = 14.56 \text{ mA} \cdot \text{cm}^{-2}$ ,  $V_{oc} = 0.74 \text{ V}$ ,  $ff = 0.68$ ) under simulated AM 1.5G irradiation ( $100 \text{ mW} \cdot \text{cm}^{-2}$ ), while other two show effective DSSCs characteristics with only around 3-4%.

## ส่วนประกอบของเนื้อความ (Content)

### 1. Introduction

In the past years, fossil fuels are the most powerful energy resources to trigger the advancement of human society. The world has been developed greatly and has utilized these powers enormously. As world population continues to grow and the availability of fossil fuels is starting to deplete, it is impossible to supply the demand of world-energy by only using fossil fuels to convert energy. This might lead to an energy and environmental crisis. At present, there are several ways to convert energy without fossil fuels, and many of them are being used, however, none of them is close to their full potential. Our country (Thailand) must take action to promote a great use of renewable energy resources, such as solar, wind, tidal energy, or nuclear power, so that we can be well prepared before the day that fossil fuels are not as abundant as they seem.

Solar energy is regarded as one of the perfect energy owing to its huge reserve, limitless, and pollution-free resources. Directly converting sun-light to electric energy based on photovoltaics is the optimal way for new generation society. Different technologies in photovoltaics, such as crystalline Si,<sup>i</sup> semiconductor (GaAs)-based cells,<sup>ii</sup> thin-film solar cells (TFSCs),<sup>iii</sup> organic bulk heterojunction (BHJ) solar cells,<sup>iv</sup> and dye-sensitized solar cells (DSSCs),<sup>v</sup> coexist to contest the future market. Among them, the DSSCs have been considered as a promising type of photovoltaic techniques because of their unique biomimetic properties.<sup>vi</sup> Although the power conversion efficiency (PCE) of dye sensitized solar cells (DSSCs) has already passed the benchmark of 10 %, a great challenge is still remained, i.e. to optimize all cell components — semiconductor, redox system, electrodes, and the sensitizer, in order to reach the maximal possible efficiency of DSSCs. To pursue this goal, investigations and developments on the sensitizer parts have found to be the greatest potential. Up to now, one deficiency of the well-established metal based Ruthenium complexes, such as the known derivatives **N3**, **N719**, **Z907** and **Black Dye**,<sup>vii</sup> is that the sunlight is absorbed in the ultraviolet-visible domain with an insufficient radiation (less intensity compared to near-infrared range in solar energy spectrum) as shown in **Figure 1**.<sup>viii</sup>

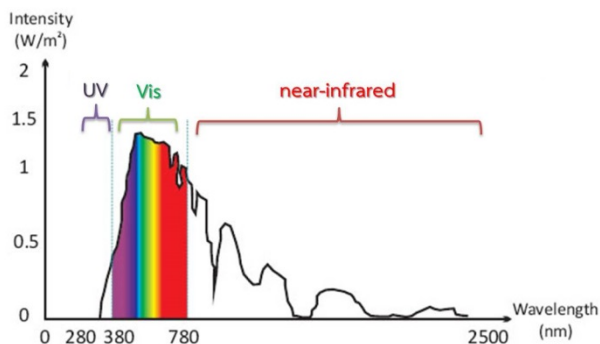


**Figure 1.** Spectrum of the solar radiation (figure was reproduced from ref.viii)

Moreover, frequent arguments against ruthenium dyes are their high cost of the rare metal ruthenium as well the limited spectral diversity of these dyes in the near-infrared (NIR) region. Therefore, alternatives for ruthenium dyes with more efficient use of the sun-light with high molar extinction coefficients together with an enlargement of the spectral diversity of the dyes towards the NIR region as well as new metal-free molecular structures are a starting point for the investigation on novel NIR organic molecular sensitizers. Among various possible designs of narrow-band-gap materials for NIR absorption,  $\pi$ -conjugated oligo-phenylenevinylene molecules are promising candidates because of their intrinsic photo-physical and redox properties. They found to have bond alternation similar to quinoidal system due to structural constraint by methylene tether. Thus these oligo-phenylenevinylene derivatives would be good candidate building blocks for absorbing long-wavelength sun-light.

Here, the development and study of heterocyclic oligo-phenylenevinylene molecules were proposed using dihydroindolo[3,2-*b*]indole as a core moiety. The synthesis and application of these derivatives will be beneficial to material science due to their thermally stable and strongly absorption in the long-wavelength sun-light.

Several reports have been published about the efficiency of dyes over 10% PCE.<sup>ix</sup> Prior to gaining the high performance of DSSCs, there are several factors for solar cell improvement such as electrolyte, the nature of dyes, counter electrode, photoelectrode, electrolyte, and interaction between components. From all elements, the structural architecture of dye sensitizer plays as the most importance role for the efficient of solar cell. Therefore, the good design of molecular dye was expected to gain high PCE.

In addition, it is also known that the modification of conjugated  $\pi$ -bridge in a push-pull dyes can shift the absorption spectrum and enhance the PCE of DSSC devices.<sup>x</sup> Organic dye **1** containing  $\pi$ -conjugated oligo-phenylenevinylene unit with electron donor-acceptor moieties was designed and synthesized by Hwang *et al.* as

displayed in **Figure 2a**.<sup>xi</sup> The conjugated bridge was aimed to facilitate intramolecular charge transfer and the anchoring of acceptor unit (commonly cyanoacrylic moiety)<sup>xii</sup> for the attachment of dye onto  $\text{TiO}_2$  nanoparticles. Even dye **1** and its derivatives exhibited the high performance of overall solar-to-electric energy conversion efficiency but there were some drawbacks owing to the  $\pi$ -bridged geometry that can distort from *cis-trans* isomerization and energy lost from the molecular rotation, which all reflex to the lesser efficiency.<sup>xiii</sup>

In 2013, Nakamura and co-workers developed organic dye **2** based on the stability of carbon-bridged phenylenevinylene (CPV) backbone (fused-ring geometry) to facilitate electron transfer within molecule (**Figure 2b**).<sup>xiv</sup> Molecular dye **2** was synthesized by introduce donor and acceptor group to provide the push-pull model with CPV as a  $\pi$ -bridged. The research efforts allowed DSSC devices based on CPV-dye **2** to reach PCE up to 7%.

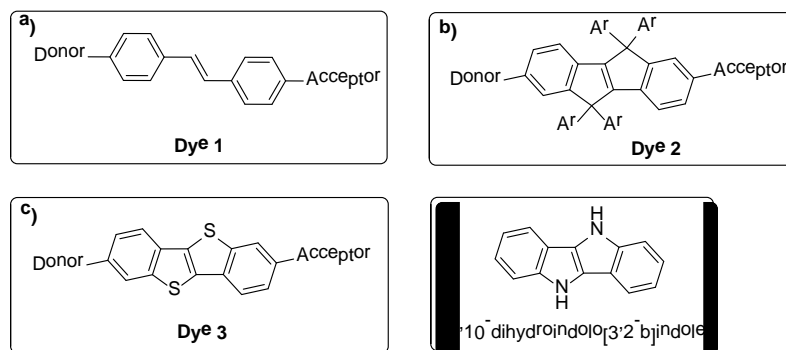


**Figure 2.** a-c) Molecular structure of organic dyes with the push-pull system (dyes **1-3**) and d) structure of nitrogen-bridged phenylenevinylene.

Recently, organic dye **3** based on [1]benzothieno[3,2-*b*]benzothiophene (BTBT) building block was designed as shown in Figure 2c and expected to improve performance of DSSC devices due to the excellent charge mobility in field-effect transistors.<sup>xv</sup> The three different electron-donating capacity groups were selected and attached with heteroaromatic backbone (BTBT) in order to assemble new chromophores with bathochromic shift. The efficiency of dye **3** series was achieved in 6.25% PCE in the presence of chenodeoxycholic acid (CDCA) as co-adsorbent for minimizing dye aggregation effects.<sup>xvi</sup> Even the gained PCE value was not as high as the best performing dyes but the morphology of BTBT building block exhibited the desirable structure of new dye family, by varying electrons donating group and modify core structure, to enhance electrical conversion energy. According to the studies mentioned above, these can provide the idea for dye structural architecture, which contained the benefit properties of dye such as high thermal stability, planar geometry (fused-ring),

and excellent electron donating capacity. Among the various research of organic dyes based on fused-ring planar structure,<sup>xvii</sup> we found that the indole derivative<sup>xviii</sup> was one of the reasonable choice that can fulfill all of the required properties and combine the advantages of fused-ring structure together with heteroaromatic compound.

The carbon-bridged or sulfur-bridged were then replaced with nitrogen atoms to provide NPV building block as depicted in **Figure 2d**. The 5,10-dihydroindolo[3,2-*b*]indole structure was capable to functionalize at the *N,N'*-positions with either alkyl or aryl group which can change the morphology of dyes in DSSC devices. The 5,10-dihydroindolo[3,2-*b*]indole was also regarded as a high electrons density compound, which can act as conjugation bridge or electron donating group. Moreover, the less steric of planar structure was expected to develop the number of organic dyes that adsorb into the  $\text{TiO}_2$  surfaces. From all described advantages the 5,10-dihydroindolo[3,2-*b*]indole core structure was expected to enhance the dye sensitized solar cell performance.

## 2. Results and discussion

The 5,10-dihydroindolo[3,2-*b*]indole dyes were designed and divided into two types, one was the double acceptors system (A-D-A: dye **4**) and another was the donor-acceptor system (D-A: dye **5** and D- $\pi$ -A: dye **6**) as shown in **Figure 3**.

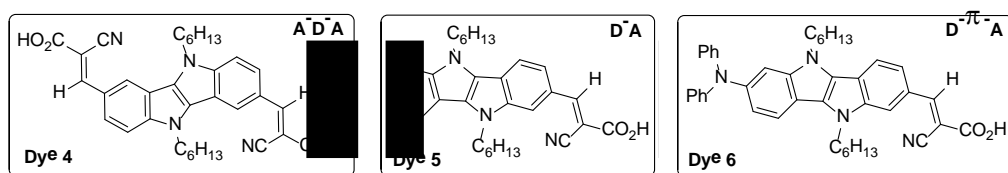
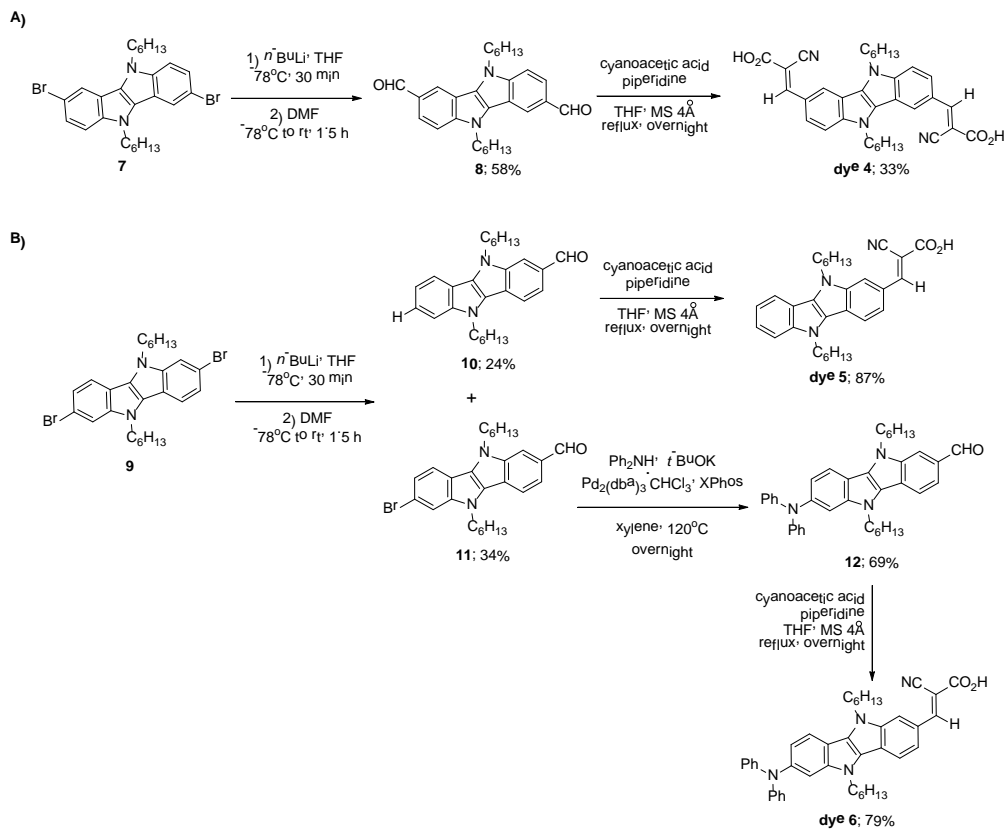


**Figure 3.** Three new structures of organic dyes **4-6** with 5,10-dihydroindolo[3,2-*b*]indole-based.

Accordingly, we have synthesized three new sensitizers by following the simple synthetic protocols as shown in Scheme 1. The newly synthesized compounds were well-characterized by  $^1\text{H}$  NMR,  $^{13}\text{C}$  NMR spectroscopy, and HRMS. The electronic and structural properties of the new dyes were investigated by UV/Vis spectroscopy while the HOMO and LUMO energy levels and hence band-gap were calculated by cyclic voltammetry and DFT studies. Further, these dyes were used to fabricate DSSCs and their photovoltaic performances were investigated.

**Synthesis of the molecular dyes.** Molecular dye **4** was prepared in 3 steps as shown in **Scheme 1A**. The compound **7** was obtained by analogy to a synthetic sequence reported earlier.<sup>xix</sup> Di-formyl compound **8** was prepared in 58% yield using lithium-halogen exchanged reaction, by treatment of the dibromo **7** with *n*-BuLi (5 equiv.) in

THF and then followed by dimethylformamide (DMF). The key step in the synthesis of dye **4** is Knoevenagel condensation. This was performed by a mixture of compound **8** refluxed in THF with cyanoacetic acid in the presence of piperidine and molecular sieve 4 $\text{\AA}$  afforded the desired product **4** in 33% yield.



**Scheme 1.** The synthesis of 5,10-dihydroindolo[3,2-*b*]indole-based dyes **4-6**.

On the other hand, molecular dyes **5** and **6** were prepared from compound **9**. The formylation reaction of compound **9** using *n*-BuLi (1.2 equiv.) gave compound **11** in moderate yield (34%) as shown in **Scheme 1B**. It was also found that lithium-hydrogen exchanged compound **10** was observed upon the reaction mixture worked-up with NH<sub>4</sub>Cl (aqueous). However it is important to note that in order to avoid diformylation formation the substrate concentration during the reaction has to be strictly controlled (0.03 mmol of compound **9** in 1 mL of THF). The Buchwald-Hartwig reaction of compound **11** and diphenylamine (DPA), catalyzed by palladium gave the compound **12** in good yield.<sup>xx</sup> Subsequent Knoevenagel condensation reaction of compound **10** and **12** with cyanoacetic acid provided molecular dyes **5** and **6**, respectively.

**Absorption and electrochemical properties.** With three dyes, the optical properties were studied using UV/Vis spectroscopic measurements. The absorption spectra of dyes **4-6** in MeOH were shown in **Figure 4** and the data were listed in **Table 1**. The spectra of dyes **4-6** exhibited two distinction absorption regions. The short one was

assigned as a  $\pi$ - $\pi^*$  transition at the wavelength of less than 340 nm, and the long one at around 350—560 nm corresponded to an intramolecular charge transfer (ICT) transition either from 5,10-dihydroindolo[3,2-*b*]indole donor (dyes **4-5**) or DPA donor to the cyanoacrylic acid acceptor. The absorption spectra of dyes **4**, **5**, and **6** are similar, but dye **4** is more red-shifted (~30 nm comparing with dye **5**) due to two electron-acceptor units while dye **6** is slightly red-shifted (~10 nm from dye **5**) as a result of an extra electron-donating effect (DPA). According to molecular orbital theory, substituted electron donating group on the *meta*-position of 5,10-dihydroindolo[3,2-*b*]indole (dye **6**) resulted in an increase in the energy of highest occupied molecular orbital (HOMO). Substituted two electron-withdrawing groups at the *para*-positions of 5,10-dihydroindolo[3,2-*b*]indole (dye **4**) was expected to decrease the energy of the lowest unoccupied molecular orbital (LUMO). Both of these substitutions decreased the energy gap between HOMO and LUMO and caused a bathochromic shift.<sup>xxi</sup> The molar extinction coefficients of these dyes were ranging from  $1.31$ — $1.85 \times 10^4 \text{ M}^{-1} \text{ cm}^{-1}$ , which were similar to that of **N719** ( $1.41 \times 10^4 \text{ M}^{-1} \text{ cm}^{-1}$ ), revealing good light harvesting nature.

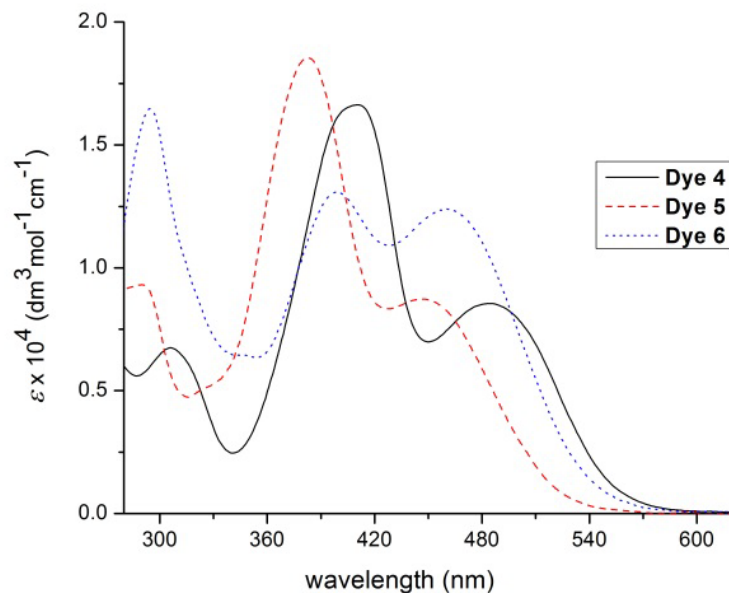


**Figure 4.** The UV/Vis spectra of dyes **4-6** in methanol.

The redox potentials of all dyes were measured by cyclic voltammetry (CV) in acetonitrile solution containing of 0.1 M tetrabutylammonium hexafluorophosphate (TBAPF<sub>6</sub>) as a supporting electrolyte, Ag/AgCl as a reference electrode, and a ferrocene/ferrocenium (Fc/Fc<sup>+</sup>) redox system as an internal standard.

**Table 1.** Photophysical and electrochemical data for dyes **4-6**.

Dye	$\lambda_{\text{abs}}^a$ (nm)	$\lambda_{\text{max}}^b$ ( $\mathcal{E} \times 10^4 / \text{dm}^3 \text{ mol}^{-1} \text{ cm}^{-1}$ )	$E_{0-0}^c$ (nm)/(eV)	$E_{\text{HOMO}}^d$ (V)	$E_{\text{LUMO}}^e$ (V)
<b>4</b>	411	1.66	564 (2.20)	1.36	-0.84
<b>5</b>	383	1.85	526 (2.36)	1.26	-1.10
<b>6</b>	403	1.31	547 (2.27)	0.96	-1.31

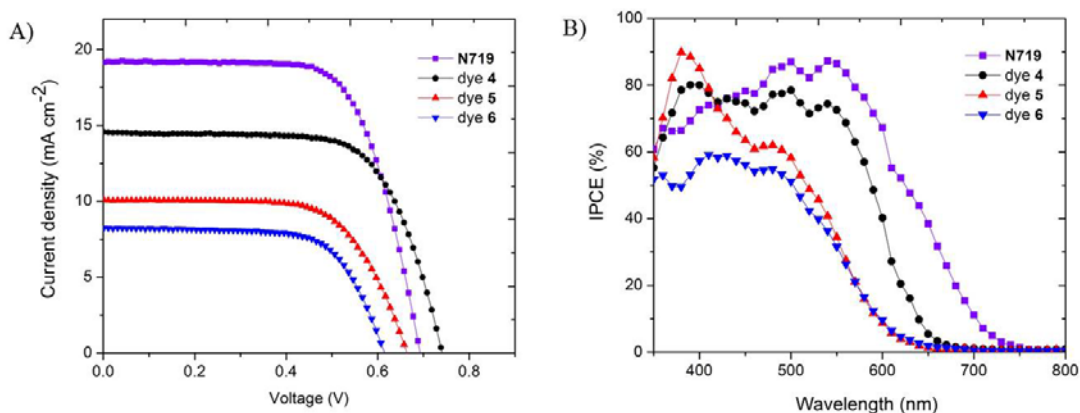
<sup>a</sup> Maximum of absorption bands in MeOH. <sup>b</sup> Extinction coefficient of the absorption band in MeOH. <sup>c</sup> Estimated from the onset of the absorption spectra in MeOH. <sup>d</sup> Oxidation potential measured vs.  $\text{Fc}^+/\text{Fc}$  in MeCN converted to NHE by adding + 0.63 V. <sup>e</sup> Estimated by  $E_{\text{ox}} - E_{0-0}$ .

The data of cyclic voltammogram were listed in **Table 1**. The first oxidation potential ( $E_{\text{onset}}$ ) was determined from the intersection of the tangent between the baseline and the current signal and the redox potential was calibrated with  $\text{Fc}^+/\text{Fc}$ <sup>xxii</sup>. The  $E_{\text{onset}}$  (see supporting information) was converted to the ground-state potential ( $E_{\text{HOMO}}$ ) by equation  $E_{\text{HOMO}} \text{ (V)} = E_{\text{onset}} \text{ (V)} + 0.63$ .<sup>xxiii</sup> By subtracting  $E_{\text{HOMO}}$  with the optical energy gap ( $E_{0-0}$ ), the corresponding excited-state potential ( $E_{\text{LUMO}}$ ) were obtained. The  $E_{\text{HOMO}}$  values of dye **4**, **5**, and **6** were estimated to be 1.36, 1.26, and 0.96 V *versus* normal hydrogen electrode (NHE), respectively. These values are more positive than the redox potential of iodide/triiodide ( $\text{I}^-/\text{I}_3^-$ ) redox mediator (0.4 V *vs.* NHE) indicating sufficient driving force for the oxidized dyes to recapture an electron from the electrolyte. The first oxidation potential of dye **6** was shift negatively by ca. 300 mV in comparison with that of dye **5**, as a consequence of the extra electron-donating group. The oxidation potentials of dye **4** and **5** are similar, revealing that the acceptor group changed on the (*meta*- or *para*-) position did not affect the potential energy level of the dyes. On the other hand, the reduction potential of dye **4** was shifted positively than dyes **5** and **6** due to an extra electron-withdrawing group of the cyanoacrylic acid. However, the LUMO levels of all dyes were higher than the  $\text{TiO}_2$  conductive band (-0.5 V *vs.* NHE), thus warranted the feasibility of electron injection.

**Performance of DSSCs.** Solar cells were fabricated by coating these dyes on the surface of  $\text{TiO}_2$  as sensitizers including the benchmark **N719** for a comparison. Their photovoltaic performances were investigated under the standard AM 1.5 G condition (100 mW  $\text{cm}^{-2}$ ). The open-circuit voltage ( $V_{\text{oc}}$ ), short-circuit current ( $J_{\text{sc}}$ ), fill factor (ff), and solar-to-electrical energy conversion efficiencies ( $\eta$ ) are summarized in **Table 2**. The  $J$ - $V$  curves of all dyes and the optimized incident photo-to-current conversion efficiencies (IPCE) are presented in **Figure 5**. The amount of dye absorbed on  $\text{TiO}_2$  films were about equal for all dyes (0.3 mM), therefore it is not regarded as a significant parameter for consideration.

**Table 2.** Photovoltaic performance of dyes.

Dye	$J_{sc}$ (mA cm <sup>-2</sup> )	$V_{oc}$ (V)	ff	$\eta$ (%)
<b>4<sup>a</sup></b>	14.56	0.74	0.68	7.39
<b>5<sup>b</sup></b>	10.09	0.66	0.66	4.44
<b>6<sup>a</sup></b>	8.25	0.62	0.68	3.44
<b>N719<sup>c</sup></b>	19.14	0.70	0.69	9.15

<sup>a</sup> 0.3 mM in MeOH:THF (1:1). <sup>b</sup> 0.3 mM in MeOH. <sup>c</sup> 0.3 mM in EtOH.**Figure 5.** A) Current-voltage ( $J$ - $V$ ) curves of DSSCs and B) The IPCE plots of DSSCs based on dyes **4**–**6** and **N719**.

From the data summarized in **Table 2**, the dye **4**-based device yielded the highest power conversion efficiency ( $\eta$ ) of 7.39 which is 81% of **N719** measured under the same condition. DSSC of dye **5** provided  $\eta$  of 4.44% whereas dye **6** gave the slightly lower  $\eta$  value of 3.44%. The overall conversion efficiency of dye **4** is higher than those of dyes **5** and **6** in an amount of ca. 40% and 47%, respectively. Furthermore, it is clear that the  $J_{sc}$  value of dye **4** is greater than those of dyes **5** and **6** as displayed in **Figure 5A**. The trend can be rationalized by the more anchoring group of cyanoacrylic group of **4**, which leads to provide more electron extraction paths compared to the congener with only one anchor. Consequently, photocurrent can be increased.<sup>xxiv</sup> The  $V_{oc}$  values of dyes are not much different from each other (0.62–0.74), nor are the filled factor of them (0.66–0.69). The  $V_{oc}$  can be partially affected by the charge recombination at  $TiO_2$ /Dye/Electrolyte interface, therefore electrochemical impedance spectral (EIS) was employed to elucidate the interfacial properties of the devices. Measurements were carried out in the dark under forward bias voltages in the XX Hz to YY Hz frequency range and bias potentials ranged from -0.60 to -0.80 V. The plots between charge recombination resistances ( $R_{CT}$ ) and applied bias voltage (V)

were shown in **Figure 6**. The values of  $R_{CT}$  exhibited trend of dye **4** (38.16  $\Omega$ ) > dye **5** (35.56  $\Omega$ ) > dye **6** (26.16  $\Omega$ ). The  $R_{CT}$  values of these dyes appeared to agree with their  $V_{oc}$  in the same order. The low  $R_{CT}$  indicates the high charge loss in the  $TiO_2$ /electrolyte interface and consequently lower  $V_{oc}$ .

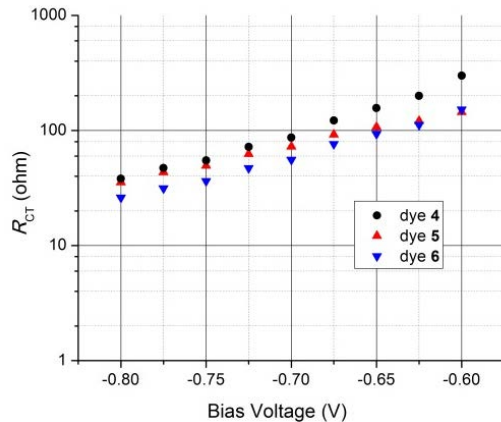


**Figure 6.** The electrochemical impedance spectral plot between charge recombination resistances ( $R_{CT}$ ) vs. applied bias voltage (V).

Furthermore, as shown in **Figure 5B**, the IPCE spectrum of dye **4** is broader than dyes **5** and **6**, which is consistent with their absorption spectra. For example, the IPCE maxima of dye **4** is approximately over 70% in the range of 425—550 nm, while at a similar IPCE level the spectral width of dye **5** is narrower (370—450 nm). For dye **6** with an extra donating group, the IPCE spectrum should be wider than that of dye **5**, as a result of a stronger resonance effect induced by the substituent. However, it showed only similar in range to dye **5** and even lower level of IPCE. This is probably due to the electron donating substitution (diphenylamine) of dye **6** retreats both the HOMO and LUMO from the NPV-bridge into the separated donor- and acceptor-parts, respectively, thereby reducing the contribution of the NPV-bridge both in the HOMO and LUMO as shown in **Figure 7**.<sup>xxv</sup>

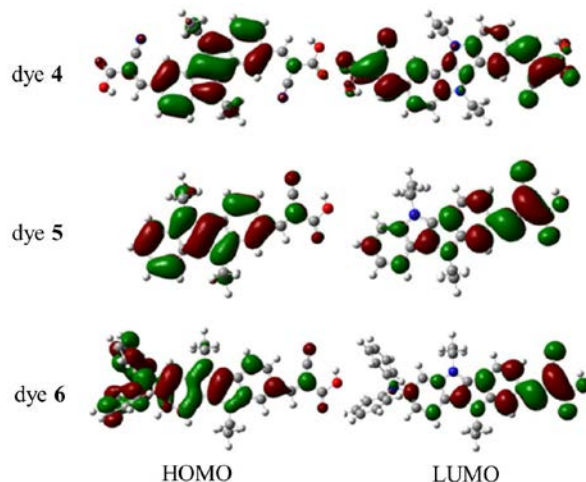


**Figure 7.** Comparison of the HOMOs (left) and LUMOs (right) of the dyes **4-6** optimized with DFT at the B3LYP/6-31 G (d) level.

**Molecular orbital calculations.** To get a basic understanding on the electronic structure of the dyes, density functional theory (DFT) were performed with B3LYP/6-31G (d) for the geometry optimization and the excited state were computed by time-dependent DFT (TD-DFT) with B3LYP functional to compare with the experimental results. The dye structures were simplified by replacing two hexyl groups with ethyl groups for maximizing the efficiency of calculation. The frontier molecular orbitals were shown in **Figure 7**. It revealed that the electron density of HOMOs are localized mainly on 5,10-dihydroindolo[3,2-*b*]indole moiety (NPV-bridge) excepting dye **6** where mostly on donating-group diphenylamine. The LUMOs of all are localized on the cyanoacrylic acid acceptor site and the adjacent NPV-bridge. The parameters of electronic transitions, *i.e.* energy, transition assignment, and oscillator strength above 0.1 were summarized (see supporting table X). In all cases, the lowest feasible transition was HOMO to LUMO charge transfer which corresponded to the lowest singlet excited state ( $S_1$ ). In addition, the computed wavelengths for both  $\pi$ - $\pi^*$  and ICT transitions were red-shifted compared to the experimental values due to negligence of the solvent effect.

**Experimental sections.** The synthesis route of compounds was shown in **Scheme 1**. Compound **7** was synthesized by the procedures reported previously. In addition, compound **9** was started with Sandmeyer reaction to provide adducts bearing bromine atoms (see supporting information).

#### **5,10-dihexyl-5,10-dihydroindolo[3,2-*b*]indole-3,8-dicarbaldehyde (8)**

In a 25 mL round-bottom flask, a solution of compound **7** (118 mg, 0.22 mmol) in anhydrous THF (3 mL) under nitrogen atmosphere was cooled down to -78 °C. Then *n*-BuLi (1.19 M, 0.94 mL, 1.12 mmol) was slowly added to the reactor and stirred at -78 °C for 30 min resulting in the yellow-brown solution. Following by the addition of anhydrous DMF (0.1 mL, 0.67 mmol) and then the reaction mixture was allowed to room temperature and stirred for another 1.5 hours. The reaction mixture was quenched with saturated NH<sub>4</sub>Cl (5 mL), extracted with ethyl acetate (20 mL×3 times), dried over anhydrous sodium sulfate. The organic layer was evaporated to provide the crude of compound **8**. The crude residue was purified by preparative thin layer chromatography ( $R_f$  = 0.69; hexanes: EtOAc; 9: 1) to yield compound **8** (55.2 mg, 0.13 mmol, 58%). <sup>1</sup>H NMR (400 MHz, acetone-d<sub>6</sub>)  $\delta$  10.14 (s, 2H), 8.05 (s, 2H), 7.97 (d, *J* = 8.2 Hz, 2H), 7.73 (d, *J* = 8.2 Hz, 2H), 4.59 (t, *J* = 7.1 Hz, 4H), 2.09–1.89 (m, 4H), 1.49–1.38 (m,

4H), 1.37–1.21 (m, 12H), 0.84 (t,  $J$  = 7.1 Hz, 6H).  $^{13}\text{C}$  NMR (101 MHz, acetone-d<sub>6</sub>)  $\delta$  192.3, 141.1, 131.4, 129.2, 120.2, 118.6, 112.0, 45.7, 31.5, 30.3, 26.8, 22.5, 13.9. HRMS (M+H)<sup>+</sup> calcd. for C<sub>28</sub>H<sub>35</sub>N<sub>2</sub>O<sub>2</sub>: 431.2699, found 431.2705.

**(2E,2'E)-3,3'-(5,10-dihexyl-5,10-dihydroindolo[3,2-*b*]indole-3,8-diyl)bis(2-cyanoacrylic acid) (dye 4)**

A mixture of compound **8** (14.6 mg, 0.03 mmol), 2-cyanoacetic acid (18 mg, 0.14 mmol) and piperidine (20  $\mu\text{L}$ , 0.20 mmol) were dissolved in anhydrous THF (3 mL) in the presence of 4 $\text{\AA}$  molecular sieve. The reaction mixture was stirred at reflux temperature for overnight under nitrogen atmosphere. After that, the reaction mixture was evaporated to dryness and the crude product was further purified by preparative thin layer chromatography ( $R_f$  = 0.15; MeOH: EtOAc; 7: 93) to yield the dye **4** (7.4 mg, 0.01 mmol, 33%).  $^1\text{H}$  NMR (400 MHz, DMSO-d<sub>6</sub>)  $\delta$  8.21 (s, 2H), 8.14 (s, 2H), 8.02 (d,  $J$  = 8.3 Hz, 2H), 7.79 (d,  $J$  = 8.2 Hz, 2H), 4.57 (m, 4H), 1.96–1.77 (m, 4H), 1.35–1.11 (m, 12H), 0.76 (t,  $J$  = 7.0 Hz, 6H).  $^{13}\text{C}$  NMR (101 MHz, DMSO-d<sub>6</sub>)  $\delta$  164.9, 149.2, 141.1, 128.2, 127.9, 120.6, 119.8, 119.4, 118.9, 114.9, 113.0, 45.7, 45.1, 31.3, 30.1, 29.4, 27.6, 26.4, 25.9, 25.2, 24.1, 22.4, 14.2. HRMS (M-H)<sup>-</sup> calcd. for C<sub>34</sub>H<sub>35</sub>N<sub>4</sub>O<sub>4</sub>: 563.2664, found 563.2332.

**5,10-dihexyl-5,10-dihydroindolo[3,2-*b*]indole-2-carbaldehyde (10) and 7-bromo-5,10-dihexyl-5,10-dihydroindolo[3,2-*b*]indole-2-carbaldehyde (11)**

In a 25 mL round-bottom flask, compound **9** (300 mg, 0.57 mmol) was stirred and cooled down to -78 °C in dry THF (20 ml), under nitrogen atmosphere. After cooling for 5 min, *n*-BuLi (1.19 M, 0.57 mL, 0.68 mmol) was slowly added to the solution mixture. After 30 min, anhydrous DMF (0.3 mL, 3.87 mmol) was added dropwise to the reaction mixture. The reaction mixture was then warmed to room temperature and stirred for additional 1.5 h. The reaction mixture was quenched with 10 mL of saturated NH<sub>4</sub>Cl, extracted with ethyl acetate, dried over anhydrous sodium sulfate, filtered and concentrated in vacuo. Crude products were obtained as a mixture of compound **10** and **11** in approximately a 1: 1 ratio. A mixture of **10** and **11** was purified by preparative thin-layer chromatography to yield compound **10** ( $R_f$  = 0.30; hexanes: EtOAc; 95: 5) in 24% (55.1 mg, 0.14 mmol).  $^1\text{H}$  NMR (400 MHz, acetone-d<sub>6</sub>)  $\delta$  10.14 (s, 1H), 8.26 (s, 1H), 8.11 (d,  $J$  = 8.2, 1H), 8.05 (d,  $J$  = 8.0 Hz, 1H), 7.74 (dd,  $J$  = 8.3, 1.3 Hz, 1H), 7.69 (d,  $J$  = 8.4 Hz, 1H), 7.41 (t,  $J$  = 7.2 Hz, 1H), 7.23 (t,  $J$  = 7.5 Hz, 1H), 4.79 (t,  $J$  = 7.1 Hz, 2H), 4.68 (t,  $J$  = 7.1 Hz, 2H), 2.08 – 1.96 (m, 4H), 1.51 – 1.32 (m, 12H), 0.95 – 0.81 (m, 6H).  $^{13}\text{C}$  NMR (101 MHz, acetone-d<sub>6</sub>)  $\delta$  192.5, 124.3, 119.7, 119.6, 119.5, 118.7,

114.0, 111.3, 46.00, 45.8, 32.3, 31.2, 31.1, 27.4, 23.3, 14.3. HRMS (M+H)<sup>+</sup> calcd. for C<sub>27</sub>H<sub>35</sub>N<sub>2</sub>O: 403.2671, found 403.2747.

And compound **11** ( $R_f$  = 0.26, hexanes: EtOAc; 95: 5) in 34% (93.3 mg, 0.19 mmol). <sup>1</sup>H NMR (400 MHz, acetone-d<sub>6</sub>)  $\delta$  10.10 (s, 1H), 8.21 (s, 1H), 8.07 (d,  $J$  = 8.3 Hz, 1H), 7.93 (d,  $J$  = 8.5 Hz, 1H), 7.87 (s, 1H), 7.71 (dd,  $J$  = 8.3, 1.3 Hz, 1H), 7.31 (dd,  $J$  = 8.5, 1.7 Hz, 1H), 4.71 (t,  $J$  = 7.1 Hz, 2H), 4.63 (t,  $J$  = 7.1 Hz, 2H), 2.02 – 1.93 (m, 4H), 1.47 – 1.25 (m, 12H), 0.84 – 0.78 (t,  $J$  = 7.2 Hz, 6H). <sup>13</sup>C NMR (101 MHz, acetone-d<sub>6</sub>)  $\delta$  192.5, 132.0, 122.5, 121.0, 119.8, 119.0, 117.4, 114.2, 45.9, 32.3, 31.2, 31.0, 27.3, 23.3, 14.3. HRMS (M+H)<sup>+</sup> calcd. for C<sub>27</sub>H<sub>34</sub>BrN<sub>2</sub>O: 481.1776, found 481.1873.

**(E)-2-cyano-3-(5,10-dihexyl-5,10-dihydroindolo[3,2-*b*]indol-2-yl)acrylic acid (dye 5)**

To a mixture of compound **10** (67.7 mg, 0.17 mmol), 2-cyanoacetic acid (53.8 mg, 0.50 mmol), and activated molecular sieves (4 Å) in 5 mL of anhydrous THF was stirred in the presence of piperidine (50 µL, 0.50 mmol) as catalyst. The reaction mixture was stirred at 80 °C for overnight under nitrogen atmosphere. After cooling temperature down and evaporating the volatile organic components, the crude residue was purified by column chromatography ( $R_f$  = 0.25; MeOH: CH<sub>2</sub>Cl<sub>2</sub>; 3: 97) to yield dye **5** (90.0 mg, 0.15 mmol, 87%). <sup>1</sup>H NMR (400 MHz, DMSO-d<sub>6</sub>)  $\delta$  8.27 (d,  $J$  = 5.1 Hz, 2H), 7.97 (d,  $J$  = 8.4 Hz, 1H), 7.93 (d,  $J$  = 7.9 Hz, 1H), 7.83 (d,  $J$  = 8.4 Hz, 1H), 7.63 (d,  $J$  = 8.4 Hz, 1H), 7.31 (t,  $J$  = 7.7 Hz, 1H), 7.15 (t,  $J$  = 7.5 Hz, 1H), 4.61 – 4.48 (m, 4H), 1.87 – 1.82 (m, 4H), 1.31 – 1.09 (m, 12H), 0.74 (td,  $J$  = 7.0, 3.1 Hz, 6H). <sup>13</sup>C NMR (101 MHz, DMSO-d<sub>6</sub>)  $\delta$  164.7, 151.0, 141.3, 139.6, 128.5, 125.7, 125.2, 123.0, 119.5, 119.4, 118.4, 117.8, 115.2, 113.4, 113.2, 110.4, 44.6, 44.4, 43.5, 30.9, 30.8, 29.72, 29.69, 25.9, 22.3, 21.9, 21.8, 13.74, 13.71. HRMS (M-H)<sup>-</sup> calcd. for C<sub>30</sub>H<sub>34</sub>N<sub>3</sub>O<sub>2</sub>: 468.2657, found 468.2422.

**7-(diphenylamino)-5,10-dihexyl-5,10-dihydroindolo[3,2-*b*]indole-2-carbaldehyde (12)**

To a mixture of compound **11** (103 mg, 0.21 mmol), XPhos (104 mg, 0.21 mmol), diphenylamine (50.6 mg, 0.21 mmol), Pd<sub>2</sub>(dba)<sub>3</sub>•CHCl<sub>3</sub> (4 mol%, 11.5 mg, 0.009 mmol), and potassium *tert*-butoxide (53.5 mg, 0.43 mmol) in 3 mL of degassed xylene was stirred under nitrogen atmosphere at 120 °C for overnight. The reaction mixture was quenched with 10 mL of saturated NH<sub>4</sub>Cl, extracted with ethyl acetate, dried over anhydrous sodium sulfate, filtered and concentrated in vacuo. A crude product was purified by preparative thin-layer chromatography ( $R_f$  = 0.25; hexanes: CH<sub>2</sub>Cl<sub>2</sub>; 6: 4) to provide compound **12** in 69% (82.6 mg, 0.14 mmol). <sup>1</sup>H NMR (400 MHz, acetone-d<sub>6</sub>)  $\delta$  10.08 (s, 1H), 8.17 (s, 1H), 7.98 (dd,  $J$  = 8.2, 3.8 Hz, 1H), 7.91 (dd,  $J$  = 8.5, 3.2 Hz,

1H), 7.67 (d,  $J$  = 8.3 Hz, 1H), 7.29 (t,  $J$  = 8.6 Hz, 5H), 7.11 (d,  $J$  = 7.6 Hz, 4H), 7.02 (t,  $J$  = 7.3 Hz, 2H), 6.92 (dd,  $J$  = 8.5, 1.4 Hz, 1H), 4.68 (t,  $J$  = 6.7 Hz, 2H), 4.44 (t,  $J$  = 6.5 Hz, 2H), 2.00 (dd,  $J$  = 15.2, 7.8 Hz, 2H), 1.91 – 1.82 (m, 2H), 1.48 – 1.39 (m, 2H), 1.36 – 1.19 (m, 10H), 0.85 – 0.76 (m, 6H).  $^{13}\text{C}$  NMR (101 MHz, acetone-d<sub>6</sub>)  $\delta$  192.3, 149.3, 145.1, 144.0, 140.6, 131.2, 130.9, 130.2, 126.6, 124.5, 123.4, 120.5, 119.8, 118.8, 118.3, 118.2, 113.8, 111.4, 107.8, 45.9, 45.6, 32.33, 32.27, 31.2, 30.9, 27.4, 27.3, 23.3, 23.2, 14.3. HRMS (M<sup>+</sup>) calcd. for C<sub>39</sub>H<sub>43</sub>N<sub>3</sub>O: 569.3406, found 569.3360.

**(E)-2-cyano-3-(7-(diphenylamino)-5,10-dihexyl-5,10-dihydroindolo[3,2-*b*]indol-2-yl)acrylic acid (dye 6)**

To a solution of compound **12** (74.0 mg, 0.13 mmol), 2-cyanoacetic acid (39.0 mg, 0.39 mmol), and activated molecular sieves (4 Å) in 5 mL of anhydrous THF was stirred for 10 min. After that, piperidine (38.5  $\mu$ L, 0.39 mmol) was slowly added and the reaction mixture was stirred overnight at 80 °C under argon atmosphere. After evaporating the volatile organic components, the crude residue was purified by column chromatography ( $R_f$  = 0.62; MeOH: CH<sub>2</sub>Cl<sub>2</sub>; 5: 95) to provide dye **6** in 79% (65.4 mg, 0.1 mmol).  $^1\text{H}$  NMR (400 MHz, DMSO-d<sub>6</sub>)  $\delta$  8.46 (s, 1H), 8.41 (s, 1H), 7.97 (q,  $J$  = 8.7 Hz, 2H), 7.90 (d,  $J$  = 8.6 Hz, 1H), 7.34 – 7.26 (m, 5H), 7.09 – 7.01 (m, 6H), 6.87 (dd,  $J$  = 8.6, 1.4 Hz, 1H), 4.56 (t,  $J$  = 6.6 Hz, 2H), 4.38 (t,  $J$  = 6.3 Hz, 2H), 1.93 – 1.84 (m, 2H), 1.77 – 1.64 (m, 2H), 1.37 – 1.14 (m, 12H), 0.81 – 0.71 (m, 6H).  $^{13}\text{C}$  NMR (101 MHz, DMSO-d<sub>6</sub>)  $\delta$  164.7, 150.9, 141.3, 139.6, 128.5, 125.7, 125.2, 122.9, 119.5, 119.4, 118.4, 117.8, 115.2, 113.4, 113.2, 110.4, 44.6, 44.4, 43.5, 30.9, 30.8, 29.7, 29.68, 25.9, 22.2, 21.9, 21.8, 13.73, 13.7. HRMS (M+Na)<sup>+</sup> calcd. for C<sub>42</sub>H<sub>44</sub>N<sub>4</sub>O<sub>2</sub>Na: 659.3362, found 659.3465.

**DSSCs device fabrication.** The photoanodes composed of nanocrystalline TiO<sub>2</sub> were prepared by using a previously reported procedure [34]. Fluorine-doped SnO<sub>2</sub> (FTO) conducting glasses (15 ohm sq<sup>-1</sup>, TEC15, Pilkington) were used for transparent conducting electrodes. The double nanostructure thick film consisting of a transparent (18NR-T, Dyesol) and a scattering (WER2-O, Dyesol) TiO<sub>2</sub> layers were screen-printed on FTO. The TiO<sub>2</sub> electrodes with cell geometry of 0.5 x 0.5 cm<sup>2</sup> were immersed in the dye solution in the dark at room temperature for 24 h to stain the dye onto the TiO<sub>2</sub> surfaces. Excess dye was removed by rinsing with appropriated solvents. The Pt counter electrode was prepared on a predrilled 8 ohm sq<sup>-1</sup>, TEC8, FTO glass (Pilkington) via the thermal decomposition of H<sub>2</sub>PtCl<sub>6</sub> solution. The dye-adsorbed TiO<sub>2</sub> photoanode and Pt counter electrode were assembled into a sealed cell by heating a gasket Meltonix 1170-25 film (25  $\mu$ m thicknesses, Solaronix) as a spacer between the electrodes. An electrolyte, 0.05 M of iodine (I<sub>2</sub>), 0.1 M of lithium iodide (LiI), 0.4 M of 4-

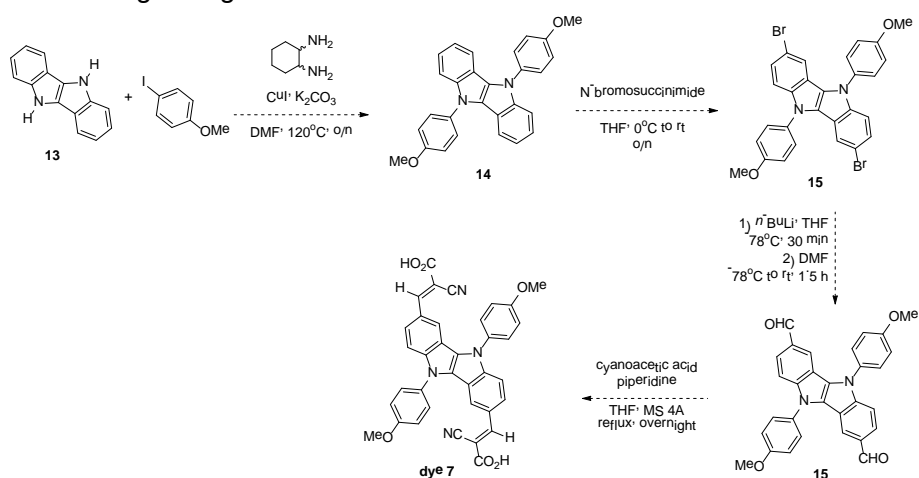
*tert*-butylpyridine (TBP), and 0.6 M of tetra-butylammonium iodide (TPAI) in a mixture of acetonitrile: veleronitrile (85: 15) were then injected through the predrilled hole by a vacuum backfilling method. The hole was sealed with a thin glass to prevent the leakage of electrolyte. Finally, the copper conducting tape and the silver paint were coated on the electrodes to enhance the electric contact.

### 3. Conclusion

We have demonstrated the design strategy and the synthesis of new dye sensitizers containing 5,10-dihydroindolo[3,2-*b*]indole as  $\pi$ -linkage (dye **6**), or as a donor with one cyanoacrylic acid group (dye **5**), and with two cyanoacrylic acid groups but varying the positions as in dye **4**. Among the three molecules, dye **4** exhibits the maximum power conversion efficiency of 7.39% ( $J_{sc} = 14.56 \text{ mA cm}^{-2}$ ,  $V_{oc} = 0.74 \text{ V}$ , ff = 0.68) under simulated AM 1.5 irradiation ( $100 \text{ mW cm}^{-2}$ ), while dyes **5** and **6** show effective DSSCs characteristics with only around 3—4%. The performance of dye **4** behaved better than those two, as a result of two anchoring groups relative to corresponding device with one counterpart.

### 4. Outlook

With these results, we plan to synthesize the anisole substituents at *N,N'*-positions instead of di-hexyl of compound **4** to enhance the donor parts of a molecule. The synthesis will start with the same procedure using dihydroindolo[3,2-*b*]indole (**13**) as shown in **Scheme 2**. The chemical, photophysical properties of compound **7** will be studied and we expect that this higher  $E_{HOMO}$  (lower energy band gap than compound **4**) will allow us to gain higher PCE.



**Scheme 2.** The synthesis of new A-D-A type with extra donor groups (anisole).

**Keywords :** Dye-sensitized solar cells, small organic dyes, indolo[3,2-*b*]indole

(คำหลัก)

**Output จากโครงการวิจัยที่ได้รับทุนจาก สกอ.**

- ผลงานตีพิมพ์ในวารสารวิชาการนานาชาติ (ระบุชื่อผู้แต่ง ชื่อเรื่อง ชื่อวารสาร ปี  
เล่มที่ เลขที่ และหน้า)  
Nopporn Ruangsupapichat,\* Metawee Ruamyart, Patcharaphon Kanchanaruggee,  
Chirapa Boonthum, Narid Prachumrak, Taweesak Sudyoadsuk, and Vinich Promarak.  
Toward rational design of metal-free organic dyes based on indolo[3,2-b]indole structure  
for dye-sensitized solar cells, Dyes and Pigments, **under revision**
- การนำผลงานวิจัยไปใช้ประโยชน์  
ยังไม่มี
- อื่นๆ ยังไม่มี

## References (ເອກສານອ້າງອີງ)

<sup>i</sup> R. B. Bergmann, *Appl. Phys. A* **1999**, 69, 187.

<sup>ii</sup> A. J. Bard, A. B. Bocarsly, F.-R. F. Fan, E. G. Walton, M. S. Wrighton, *J. Am. Chem. Soc.* **1980**, 102, 3671.

<sup>iii</sup> Y. Hamakawa (Ed.) *Thin-Film Solar Cells: Next Generation Photovoltaics and Its Applications*, Springer Series in Photonics, New York, USA, **2004**.

<sup>iv</sup> J. Roncali, *Acc. Chem. Res.* **2009**, 42 (11), 1719.

<sup>v</sup> M. Grätzel, *Journal of Photochemistry and Photobiology C: Photochemistry Reviews* **2003**, 4, 145.

<sup>vi</sup> B. O'Regan, M. Grätzel, *Nature* **1991**, 353, 737.

<sup>vii</sup> A. Albini, *Photochemistry*, RSC Publishing, **2011**, 39, 112.

<sup>viii</sup> E. V. Appleton, *Nature* **1945**, 156, 535.

<sup>ix</sup> a) Zeng, W.; Cao, Y.; Bai, Y.; Wang, Y.; Shi, Y.; Zhang, M.; Wang, F.; Pan, C.; Wang, P. *Chem. Mater.* **2010**, 22, 1915. b) Zhou, N.; Prabakaran, K.; Lee, B.; Chang, S. H.; Harutyunyan, B.; Guo, P.; Butler, M. R.; Timalsina, A.; Bedzyk, M. J.; Ratner, M. A.; Vegiraju, S.; Yau, S.; Wu, C.-G.; Chang, R. P. H.; Facchetti, A.; Chen, M.-C.; Marks, T. J. *J. Am. Chem. Soc.* **2015**, 137, 4414.

<sup>x</sup> T. Gaiger, S. Kuster, J.-H. Yum et al. *Advance Functional Materials* **2009**, 19, 2720.

<sup>xi</sup> Hwang, S.; Lee, J. H.; Park, C.; Lee, H.; Kim, C.; Park, C.; Lee, M.-H.; Lee, W.; Park, J.; Kim, K.; Park, N.-G.; Kim, C. *Chemical Communications* **2007**, 46, 4887.

<sup>xii</sup> a) Chen, Y.-F.; Liu, J.-M.; Huang, J.-F.; Tan, L.-L.; Shen, Y.; Xiao, L.- M.; Kuanga, D.-B.; Su, C.-Y. *J. Mater. Chem. A* **2015**, 3, 8083. b) Lee, M.-W.; Kim, J.-Y.; Lee, D.-H.; Ko, M. J. *ACS Appl. Mater. Interfaces* **2014**, 6, 4102. c) Li, X.; Zheng, Z.; Jiang, W.; Wu, W.; Wang, Z.; Tian, H. *Chem. Commun.* **2015**, 51, 3590. d) Qian, X.; Gao, H.-H.; Zhu, Y.-Z.; Lu, L.; Zheng, J.-Y. *J. Power Sources* **2015**, 280, 573. e) Huang, Z.-S.; Cai, C.; Zang, X.-F.; Iqbal, Z.; Zeng, H.; Kuang, D.-B.; Wang, L.; Meier, H.; Cao, D. *J. Mater. Chem. A* **2015**, 3, 1333. f) Yang, L.-N.; Li, S.-C.; Li, Z.-S.; Li, Q.-S. *RSC Adv.* **2015**, 5, 25079. g) Dessì, A.; Calamante, M.; Mordini, A.; Peruzzini, M.; Sinicropi, A.; Basosi, R.; Fabrizi de Biani, F.; Taddei, M.; Colonna, D.; Di Carlo, A.; Reginato, G.; Zani, L. *Chem. Commun.* **2014**, 50, 13952.

<sup>xiii</sup> (a) C. Kim, H. Choi, S. Kim, C. Baik, K. Song, M.-S. Kang, S. O. Kang and J. Ko, *J. Org. Chem.*, **2008**, 73, 7072; (b) Y.-D. Lin and T. J. Chow, *J. Mater. Chem.*, **2011**, 21, 14907.

<sup>xiv</sup> X. Zhu, H. Tsuji, A. Yella, A. S. Chauvin, M. Grätzel, E. Nakamura, *Chem. Commun.* **2013**, 49, 582.

<sup>xv</sup> a) Takimiya, K.; Ebata, H.; Sakamoto, K.; Izawa, T.; Otsubo, T.; Kunugi, Y. *J. Am. Chem. Soc.* **2006**, 128, 12604. b) Ebata, H.; Izawa, T.; Miyazaki, E.; Takimiya, K.; Ikeda, M.; Kuwabara, H.; Yui, T. *J. Am. Chem. Soc.* **2007**, 129, 15732. c) Izawa, T.; Miyazaki, E.; Takimiya, K. *Adv. Mater.* **2008**, 20, 3388.

<sup>xvi</sup> Capodilupo, A. L.; Fabiano, E.; De Marco, L.; Ciccarella, G.; Gigli, G.; Martinelli, C.; Cardone, A., *J Org Chem* **2016**, 81 (8), 3235.

---

<sup>xvii</sup> a) Chu, B.; Wang, H.; Xerri, B.; Lee, K.-H.; Yang, T.; Wang, Z.; Lin, Z.; Liang, Y.; Adamo, C.; Yang, S.; Sun, J. *RSC Adv.* **2014**, *4*, 62472. b) Yang, L.; Zheng, Z.; Li, Y.; Wu, W.; Tian, H.; Wang, Z. *Chem. Commun.* **2015**, *51*, 4842. c) Huang, Z.-S.; Feng, H.-L.; Zang, X.-F.; Iqbal, Z.; Zeng, H.; Kuang, D.-B.; Wang, L.; Meierd, H.; Cao, D. *J. Mater. Chem. A* **2014**, *2*, 15365. d) Choi, H.; Shin, M.; Song, K.; Kang, M.-S.; Kang, Y.; Ko, J. *J. Mater. Chem. A* **2014**, *2*, 12931.

<sup>xviii</sup> a) Xue-Hua Zhang, Yan Cui, Ryuzi Katoh, Nagatoshi Kourumura,\* and Kohjiro Hara\* *J. Phys. Chem. C* **2010**, *114*, 18283. b) Su, J.-Y.; Lo, C.-Y.; Tsai, C.-H.; Chen, C.-H.; Chou, S.-H.; Liu, S.-H.; Chou, P.-T.; Wong, K.-T. *Org. Lett.* **2014**, *16*, 3176. c) Dickson D. Babu a , Saritha Reddy Gachumale b , Sambandam Anandan b , Airody Vasudeva Adhikari a Dyes and Pigments **2015**, *112*, 183. d) Dickson D. Babu a, c , Rui Su b , Praveen Naik c , Ahmed El-Shafei b, \*\*, Airody Vasudeva Adhikari c, \* *Dyes and Pigments* **2017**, *141*, 112.

<sup>xix</sup> Youngeup Jin, K. K., Suhee Song, Jinwoo Kim, Jaehong Kim, Sung Heum Park, Kwanghee Lee, Hongsuk Suh, New Conjugated Polymer Based on Dihydroindoloindole for LEDs. *Bulletin of the Korean Chemical Society* **2006**, *27* (7), 1043.

<sup>xx</sup> J. Yin, S. L. Buchwald, *J. Am. Chem. Soc.* **2002**, *124*, 6043.

<sup>xxi</sup> J. Hung, W. Liang, J. Luo, Z. Shi, A. K. Y. Jen, X. Li, *Journal of Physical Chemistry C* **2010**, *114*, 22284.

<sup>xxii</sup> Agrawal, A. K. Jenekhe, S. A. *Chemistry of Materials*, **1996**, *8*, 579.

<sup>xxiii</sup> X. Jiang, K. M. Karlsson, E. Gabrielson, E. M. J. Johansson... *Advance Functional Materials*, **2011**, *21*, 2944.

<sup>xxiv</sup> N. Manfredi, B. Cecconi and A. Abbotto, *Eur. J. Org. Chem.*, **2014**, 7069.

<sup>xxv</sup> A. Mishra, M. K. R. Fisher, P. Bauerle, *Angew. Chem. Int. Ed.* **2009**, *48*, 2474.